



Flow pattern transition models and correlations for flow boiling in mini-tubes



Mohamed M. Mahmoud^{a,b}, Tassos G. Karayiannis^{a,*}

^a School of Engineering and Design, Brunel University London, Uxbridge UB8 3PH, UK

^b Faculty of Engineering, Zagazig University, Zagazig 44519, Egypt

ARTICLE INFO

Article history:

Received 11 February 2015

Received in revised form 17 September 2015

Accepted 19 September 2015

Available online 26 September 2015

Keywords:

Flow boiling

Mini tubes

Flow patterns

Correlations

ABSTRACT

An evaluation of models and correlations predicting flow patterns in mini-tubes is described in this paper and final recommendations are made for a way forward. Flow boiling patterns of R245fa in a 1.1 mm diameter copper tube were used in this evaluation. The experiments covered an experimental range of mass flux 100–400 kg/m² s, heat flux 3–25 kW/m², inlet pressure of 1.85 and inlet subcooling of 5 K. Hysteresis was evident in these experiments across the whole range, with obvious changes in the flow patterns between increasing and decreasing heat flux. The four main flow patterns were bubbly, slug, churn and annular flow. Confined flow was also evident. For increasing heat flux, only annular flow was evident but all the flow patterns were evident with decreasing heat flux. Therefore, the evaluation of flow pattern maps carried out in this study was based on the decreasing heat flux data, as this covered the full range of flow patterns. The evaluation of more than ten models and correlations demonstrated that there is no general model that can predict accurately all flow pattern transition boundaries. Only one model succeeded in predicting all transition boundaries very well, except the bubbly to slug transition. Thus, a new modification on this boundary is proposed in this paper that could predict the experimental data used in this study very well.

© 2015 The Authors. Published by Elsevier Inc. This is an open access article under the CC BY license (<http://creativecommons.org/licenses/by/4.0/>).

1. Introduction

The application of flow boiling in microchannels as a cooling method of high heat flux devices is of great interest to the engineering community. Progress is currently restricted by a limited knowledge of flow patterns and subsequent heat transfer mechanisms and the ability to predict pressure drop and heat transfer rates. A recent review by Mahmoud et al. [1] is available, which includes a section on past work on flow patterns in small to micro diameter tubes. This review demonstrates that: (i) channel size has a significant effect on the morphology of gas–liquid two phase flow, (ii) the most frequently identified flow patterns are bubbly, slug, churn and annular flow with confined bubble flow evident in certain operating ranges, (iii) dispersed bubbly, churn and stratified flow tend to diminish as the diameter decreases. Flow pattern maps and prediction methods are available in literature but these are often restricted to particular experimental conditions and certain fluids. Hassan et al. [2] found large discrepancies in the reported flow patterns in microchannels when previous experimental flow maps were compared against each other. Additionally,

they found that channel orientation affects the transition boundaries although many researchers reported insignificant effect. Thus, they proposed two universal maps, one for horizontal and one for vertical channels. The limitation in the development of new accurate flow pattern maps could be attributed to the reasons discussed below.

The first reason is the lack of understanding all the parameters which could affect the flow patterns. Shao et al. [3] thought that the dominating factors for flow pattern transitions are channel size, superficial velocities, liquid phase surface tension and channel wettability. Evaluation of past literature can reveal that there are contradictions among researchers on the effect of these factors. For example, some researchers such as [4–7] agreed on that the transition to annular flow shifts to higher gas superficial velocities as the diameter decreases while researchers [8,9] reported an opposite effect. Some researchers investigated the effect of contact angle (surface wettability) on flow patterns characteristics in macro and microchannels, see for example [10–14]. The definition of contact angle and surface wettability is depicted in Fig. 1. They agreed on that surface wettability has a significant effect on flow patterns. All conventional flow patterns (bubbly, slug, churn, annular) were reported to occur in the highly wetting channels investigated in their study, i.e. $\theta = 7\text{--}45^\circ$ [10–14]. As contact angle

* Corresponding author.

E-mail address: tassos.karayiannis@brunel.ac.uk (T.G. Karayiannis).

Nomenclature

Bd	bond number (-), $g\Delta\rho D^2/\sigma$	u_d	drift velocity (m/s)
Bo	boiling number (-), q/Gh_{fg}	u_{gs}	gas superficial velocity (m/s)
C_0	distribution parameter	u_h	homogeneous velocity (m/s), $u_h = u_{gs} + u_{ls}$
Ca	capillary number (-), $Ca = \mu u/\sigma$	u_l	liquid velocity defined by Eq. (20)
Co	confinement number (-), $\frac{1}{D}\sqrt{\sigma/g\Delta\rho}$	u_{ls}	liquid superficial velocity (m/s)
c_1	experimental coefficient for critical void fraction on bubbly slug boundary, Eq. (16)	U_g	actual gas velocity (m/s)
c_2	experimental exponent for critical void fraction on bubbly-slug boundary, Eq. (16)	U_l	actual liquid velocity (m/s)
D	tube diameter (m)	U_r	relative velocity, ($U_g - U_l$)
D_b	bubble diameter (m)	We_b	Weber number based on bubble diameter and homogeneous velocity, $We_b = \rho_g u_h^2 d_c/\sigma$
d_c	critical bubble diameter, Eq. (21) (m)	We_{gs}	Weber number based on gas superficial velocity, $We_{gs} = \rho_g u_{gs}^2 D/\sigma$
d_{max}	maximum bubble diameter (m)	We_{ls}	Weber number based on liquid superficial velocity, $We_{ls} = \rho_l u_{ls}^2 D/\sigma$
$(d_{max})_0$	maximum bubble diameter for dilute dispersion (m)	We_g	gas Weber number based on total mass flux, $We_g = G^2 D/\rho_g \sigma$
$(d_{max})_z$	maximum bubble diameter for denes dispersion (m)	We_l	liquid Weber number based on total mass flux, $We_l = G^2 D/\rho_l \sigma$
Eo	Eotvos number (-), $g\Delta\rho D^2/8\sigma$	We_r	liquid Weber number based on the relative actual velocity, Eq. (38)
Fr_{gs}	Froude number based on gas superficial velocity, $Fr_{gs} = u_{gs}/\sqrt{gD}$	x	horizontal axis (-)
Fr_{gs}^*	modified Froude number based on gas superficial velocity, $Fr_{gs}^* = u_{gs}\sqrt{\rho_g/(\rho_l - \rho_g)gD}$	x_e	exit vapor quality (-)
f_l	friction factor based on homogeneous velocity	$x_{IB/CB}$	vapor quality at the transition from isolated bubble to coalescing bubble regime
g	gravitational acceleration (m/s ²)	$x_{CB/A}$	vapor quality at the transition from coalescing bubble to annular regime
G	mass flux (kg/m ² s)	y	vertical axis (-)
k	Constant in Eq. (5)		
K	Constant in Eq. (20)		
P	pressure (Pa)		
P_g	gas pressure (Pa)		
P_l	liquid pressure (Pa)		
q	heat flux (W/m ²)		
Re_{go}	Reynolds number based on all flow as gas, $Re_{go} = GD/\mu_g$		
Re_{gs}	Reynolds number based on gas superficial velocity, $Re_{gs} = \rho_g u_{gs} D/\mu_g$		
Re_h	Reynolds number based on homogeneous velocity, $Re_h = \rho_l u_h D/\mu_l$		
Re_{lo}	Reynolds number based on all flow as liquid, $Re_{lo} = GD/\mu_l$		
Re_{ls}	Reynolds number based on liquid superficial velocity, $Re_{ls} = \rho_l u_{ls} D/\mu_l$		
Su	Suratman number, $Su = Re_{ls}/Ca_{ls}$		
T_{sat}	Saturation temperature (°C)		

Greek symbols

α	void fraction
α_{act}	actual void fraction
α_{cal}	calculated void fraction, $u_{gs}/(u_{gs} + u_{ls})$
α_c	critical void fraction
θ	contact angle (°)
μ_g	gas dynamic viscosity (kg/m s)
μ_l	liquid dynamic viscosity (kg/m s)
ρ_g	gas density (kg/m ³)
ρ_l	liquid density (kg/m ³)
σ	surface tension (N/m)

increases (low wettability), the liquid film around the slug becomes thicker and unstable resulting in a new pattern called rivulet flow, which replaces churn flow. On the contrary, Wang et al. [15] reported that reducing surface wettability (increasing θ) did not induce the appearance of new flow patterns. They reported slug, slug-annular, annular and parallel flow (stratified) within a contact angle range $\theta = 37\text{--}135^\circ$.

Another example of contradiction found in the literature, is the effect of surface tension. Some researchers such as [6,7,15–17] agreed that the transition lines shift to lower gas superficial velocities as surface tension decreases. On the contrary, researchers [18,19] reported an opposite effect. Moreover, the contradiction on the relative importance of the above factors, i.e. wettability and surface tension, can also be detected from the various coordinates used for plotting the flow maps. For example, researchers [2,16,20] plotted their maps as a function of the superficial liquid and gas velocities. This means that the effect of other parameters such as wettability, surface tension, viscosity, density is not included. Other researchers such as [6,21] plotted their maps as a function of liquid and gas Weber numbers, which consider the effect of diameter, velocity, density and surface tension.

The second reason is the fact that developing accurate flow maps and transition models requires a large databank of results with varying fluid properties, channel size and experimental conditions. This is currently hindered by the discrepancies found in the available data as discussed above, even when using the same refrigerant and channel diameter. Karayiannis et al. [22] suggested that these discrepancies were due to the surface characteristics and heated length. As indicated by Consolini et al. [23], flow stability was also an important factor. A study by Mahmoud et al. [24] into the effects of surface characteristics using seamless and

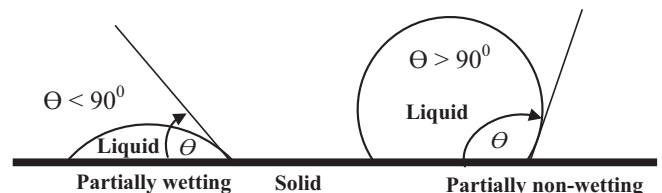


Fig. 1. Definition of surface wettability and contact angle (θ).

Download English Version:

<https://daneshyari.com/en/article/7052084>

Download Persian Version:

<https://daneshyari.com/article/7052084>

[Daneshyari.com](https://daneshyari.com)